

See discussions, stats, and author profiles for this publication at: <https://www.researchgate.net/publication/228501687>

Mesoscopic Modelling of Fluid Flows in Micro and Nano Channel

Article in *International Journal of Modern Physics C* · March 2007

DOI: 10.1142/S0129183107011029

CITATION

1

5 authors, including:



Luca Biferale

University of Rome Tor Vergata

280 PUBLICATIONS **5,837** CITATIONS

[SEE PROFILE](#)



Mauro Sbragaglia

University of Rome Tor Vergata

116 PUBLICATIONS **2,432** CITATIONS

[SEE PROFILE](#)



Sauro Succi

INFN - Istituto Nazionale di Fisica Nucleare

551 PUBLICATIONS **17,802** CITATIONS

[SEE PROFILE](#)



Federico Toschi

Technische Universiteit Eindhoven

282 PUBLICATIONS **5,758** CITATIONS

[SEE PROFILE](#)

Some of the authors of this publication are also working on these related projects:



Graphene oxide for environmental applications [View project](#)



Turbulence [View project](#)

International Journal of Modern Physics C
© World Scientific Publishing Company

MESOSCOPIC MODELLING OF FLUID FLOWS IN MICRO AND NANO CHANNEL.

Roberto Benzi, Luca Biferale

*Dip. Physics and INFN, Univ. Roma "Tor Vergata", Address
via della Ricerca Scientifica 1, 00133, Roma, *
benzi@roma2.infn.it*

Mauro Sbragaglia

*Department of Applied Physics, University of Twente, Address
P.O. Box 217, 7500 AE Enschede, The Netherlands*

Sauro Succi, Federico Toschi

*Istituto per le Applicazioni del Calcolo CNR, Address
Viale del Policlinico 137, 00161 Roma, Italy.*

Received Day Month Year

Revised Day Month Year

We review some recent results in the theory of Lattice Boltzmann Equation applied in micro and nano channel flows. With a suitable generalization of the Shan-Chan model, we are able to relate in a systematic and self consistent way, the model parameters with the contact angle. Comparison with Molecular Dynamics simulations show remarkable agreement.

Keywords: Two Phase Flows; Nano fluids

PACS Nos. 83.50.Rp,68.03.Cd.,0520.Dd,02.70.Ns

1. Introduction.

The last 30 years have witnessed the emergence of a growing body of knowledge on complex systems, i.e. systems whose macroscopic behaviour is difficult to characterize even though their microscopic dynamics is generally well understood. Remarkable examples of complex systems are turbulent flows, glassy systems, material fractures. In most cases, beside the traditional experimental and theoretical work, numerical simulations have played an important role as a valuable tool for investigating the statistical and dynamical properties of complex systems. The role of numerical simulations is to help us in building a systematic conceptual framework

*State completely without abbreviations, the affiliation and mailing address, including country. Typeset in 8 pt italic.

2 *R. Benzi, L. Biferale, M. Sbragaglia, S. Succi, F. Toschi*

for extracting macroscopic dynamics from microscopic laws. From this point of view, the Lattice Boltzmann Equation (LBE) has been shown to provide a new and important tool in understanding mesoscopic dynamics and in helping us to investigate many complex systems related to fluid flows. The basic idea behind LBE^{1,2,3} is to forget about the detailed molecular laws underlying fluid flows (i.e. the lattice gas dynamics) and to introduce a suitable mesoscopic modeling.

Recent experimental results for flows in micro and nano channels have shown new and unexpected results which, so far, have been reproduced solely by using molecular dynamics (MD). Molecular dynamics, however, cannot simulate macroscopic systems for long enough time, i.e. systems with the same spatial and temporal scales of real experiments. It is therefore a challenging question whether a suitable version of LBE can correctly reproduce the relevant physical behaviour observed in micro and nano flows with complex wetting and dewetting properties. The aim of this paper is to review recent advances in this direction.

2. The model.

The simplest LBE reads as follows⁴:

$$f_\alpha(\mathbf{x} + \mathbf{c}_\alpha \Delta t, t + \Delta t) - f_\alpha(\mathbf{x}, t) = -\omega \Delta t [f_\alpha(\mathbf{x}, t) - f_\alpha^{(eq)}(\mathbf{x}, t)] + F_\alpha \Delta t, \quad (1)$$

where $f_\alpha(\mathbf{x}, t)$ is the probability of finding a particle at site \mathbf{x} at time t , moving along one of the α -th lattice direction defined by the discrete speed \mathbf{c}_α with $\alpha = 1, \dots, b$ and Δt is the time unit. The left-hand side of (1) stands for molecular free-streaming, whereas the right-hand side represents molecular collisions. These are expressed through a simple relaxation towards local Maxwellian equilibrium $f_\alpha^{(eq)}$ in a time lapse of the order of $\tau \equiv \omega^{-1}$. Finally, the term F_i represents a volumetric body-force, which can be tailored to produce non-trivial macroscopic effects, such as phase-transitions. Non-ideal effects, leading to two-phase flows, are modeled through a self-consistent force term:

$$\mathbf{F}(\mathbf{x}, t) = -\mathcal{G}_b \sum_{\alpha} w_\alpha \psi(\mathbf{x}, t) \psi(\mathbf{x} + \mathbf{c}_\alpha \Delta t, t) \mathbf{c}_\alpha. \quad (2)$$

Here, $\psi(\mathbf{x})$ is a phenomenological pseudo-potential (generalized density), $\psi(\mathbf{x}, t) = \psi[\rho(\mathbf{x}, t)]$, first introduced by Shan and Chen⁵, w_i are normalization weights and \mathcal{G}_b tunes the molecule-molecule interaction, i.e. it plays the role of the normalized *inverse temperature*, ϵ/KT , with ϵ the molecular interaction, K the Boltzmann constant and T the system temperature. In the following, we choose the standard form $\psi = \sqrt{\rho_c} \{1 - \exp(-\rho/\rho_c)\}$, with the reference density $\rho_c = 1$, in lattice units.

The interaction potential (2) can be regarded as the simplest “mean-field” approximation of the body force induced by soft particle-particle interactions in the collisional term of the Boltzmann Equations⁶.

In spite of its simplicity, the Shan-Chen approach provides two crucial ingredients of non-ideal fluid behavior: a non-ideal equation of state and a non-zero liquid-vapor surface tension, σ_{lv} . Both features are encoded in the expression of the

non-ideal momentum flux tensor P_{ij} . In the hydrodynamic limit, the LBE equations (1)-(2) can be shown to evolve according to the Navier-Stokes equations⁶, with the following pressure tensor \overleftrightarrow{P} :

$$P_{ij} = \left[c_s^2 \rho + \frac{1}{2} c_s^2 \mathcal{G}_b \psi^2 + \frac{1}{2} c_s^4 \mathcal{G}_b \psi \Delta \psi + \frac{\mathcal{G}_b c_s^4}{4} |\nabla \psi|^2 \right] \delta_{ij} - \frac{1}{2} c_s^4 \mathcal{G}_b \partial_i \psi \partial_j \psi. \quad (3)$$

This is the basic equation for understanding the effect of surface tension between the two different phases of the system. The surface tension can be obtained as an integral of the mismatch of the normal and transverse component of the $P_{i,j}$, along the coordinate normal to the surface of the interface. Following⁵ and the above definition, one can show that the surface tension between liquid and vapor is given by:

$$\sigma_{lv} = -\frac{1}{2} c_s^4 \mathcal{G}_b \int |\partial_y \psi|^2 dy$$

where we assume the only dependence to be on the y direction.

However, σ_{lv} does not characterize the wetting properties of the fluid. To do so we need to introduce the interaction of the fluid with the boundary. The main idea is to introduce a reference density ρ_w which must be matched by $\rho(\mathbf{x})$ at the wall, i.e. we assume $\psi_w = \psi(\rho_w)$, where ρ_w should be regarded as a free-parameter related to the strength of the fluid/solid interactions. Also, we assume bounce back boundary conditions for the f_α at the wall. In figure (1) we show the results of a 2D numerical simulations with different average density $\langle \rho \rangle$, where the average is performed over the stream wise direction of the channel. In both cases represented in figure (1) the interaction of the fluid with the wall is parameterized by the same ρ_w . As a consequence, for relatively small $\langle \rho \rangle$ a thin layer of “gas” develops near the boundary, changing the wetting properties of the flows.

The above discussion tells us the wetting properties of fluid, usually parameterized in terms of *contact angle*, must be a function of the parameter ρ_w , i.e. on the interaction of the fluid with the boundary. In⁶, it has been shown that by imposing the condition of mechanical equilibrium, $\partial_j P_{ij} = 0$, of the contact line separating the liquid, vapor and solid phases, one can compute analytically the *contact angle*, $\theta(\mathcal{G}_b, \rho_w)$.

The result is:

$$\cos(\theta) = \frac{\int_{sv} |\partial_y \psi|^2 dy - \int_{sl} |\partial_y \psi|^2 dy}{\int_{lv} |\partial_y \psi|^2 dy} \quad (4)$$

where $\int_{sl} |\partial_y \psi|^2 dy$, $\int_{sv} |\partial_y \psi|^2 dy$, $\int_{lv} |\partial_y \psi|^2 dy$ indicate the positive integrals calculated along the solid-liquid, solid-vapor and liquid-vapor interfaces with y the coordinate normal to the interface. A direct check of equation (4) is presented in figure (2), where the line is the theoretical prediction from (4) while the points represents direct “measurements” obtained by numerical simulations.

4 *R. Benzi, L. Biferale, M. Sbragaglia, S. Succi, F. Toschi*

Notwithstanding their inherently mesoscopic character, the parameters \mathcal{G}_b and ρ_w carry no less physical content than their atomistic counterparts (relative strength of the attractive to repulsive interactions in MD simulations ^{7,8,9}). It should be emphasized that the contact angle can be computed also within the framework of the free-energy version of the lattice Boltzmann method for non-ideal fluids ^{10,11}. Here, however, we prefer to stick to the Shan-Chen pseudo-potential formulation, because of its simplicity.

3. Benchmark against analytical results.

One of the consequences of large contact angles is that the flow can show apparent slipping, i.e. the velocity profile follows the usual parabolic profile up to a relatively thin layer near the boundary. One can compute an apparent slip length λ_{eff} by extrapolating the parabolic profile to cross the zero velocity line (inside the wall). There are very few analytical prediction on the slip length (as previously defined) with respect to the contact angle.

Let us consider a Poiseuille flow in a three dimensional channel with x the streamwise direction and y the spanwise direction, confined between two plates at $z = 0$ and $z = L_z$. The two plates are supposed to be a mixture of complete wetting and complete dewetting material. In particular we consider two possible geometries: 1) strips of wide H in the x direction and 2) strips of wide H in the y direction. Let us denote L_x and L_y the streamwise and spanwise dimension of the channel and $\xi \equiv H/L$ where L stands for L_x or L_y for the two cases. In ¹², the problem referring to case 1) was solved analytically and recently in ¹³, an analytical solution was provided also for case 2). In both cases, one is able to compute the effective slip length as a function of the relevant parameter ξ . It is worthwhile to understand whether our model does meet the analytical results for the same geometry of alternating no-slip (complete wetting and contact angle equal 0) and free slip (complete dewetting and contact angle 180°) boundary conditions. The comparison is done in figure (3) where the lines represent the analytical solutions, for the two different cases, and points are the results of our numerical 3D simulations. In both cases we used bounce back boundary conditions for the LBE populations. As one can see, the agreement is extremely good.

4. LBE versus molecular dynamics.

As discussed in the introduction, MD played an important role in understanding the physics of slip phenomena in nano channel. One particular interesting case ¹⁴ ¹⁵ is provided by the MD simulations with boundary conditions showing a groove (see insert in figure (4)). This is a quite different situation with respect to that analyzed in the previous section. While in figure (3) the analytical and numerical results have been obtained for *plane* surfaces with different wetting properties, here we consider a relatively complex geometry (i.e. the “groove” represented in figure (4)) with introduces capillary effects. The upper part of the system has zero contact

angle (complete wetting) while the lower part (including the groove) has a contact angle near 135° .

For different “bulk” pressure, the groove induces a non trivial capillary effect. In particular, at relatively large pressure the flow is able to wet all the system. By decreasing the pressure two things happen: first the fluid does not wet the groove and next, the fluid does not wet all the lower boundary. In figure (4) we show the MD simulations (circles) representing the “state of the system” in the following coordinate: $\Delta P_{lv} \equiv P - P_c$ i.e. pressure computed with respect to the capillary pressure and d/L_x which is the distance of the upper boundary to the top of the groove measured in terms of L_x , the length of the box. By changing the parameter d/L_x (somehow proportional to the density) we can change the pressure of the system. The plateau observed in figure (4) corresponds to the dewetting of the groove (as indicated by the arrow). In summary, the presence of the groove enhance the slipping properties of the flow. In figure (4) we compare the MD simulations (circles) with LBE simulations (squares) using the model previously described. Note that by fixing the contact angle there is no free parameter in the LBE simulations. As one can see, we obtain a rather excellent agreement between the two simulations. This our most important result and indicates the possibility to correctly represent the complex wetting and dewetting properties by using an appropriate mesoscopic model, i.e. the LBE model used so far.

The interaction between the geometrical properties of the boundary and the thermodynamical properties of the fluid can be highly non trivial. As a preliminary examples, we show in figure (5) the case of two grooves (not equally spaced). With respect to figure (4), nothing has been changed expect the geometry. The pressure/density diagram of figure (5) shows a “two state” system. It is worth mentioning that the result shown in figure (4) and (5) open the way to numerical simulations on micro and nano flows with realistic space and time scales, compared with laboratory experiments.

References

1. R. Benzi, S. Succi & M. Vergassola *Phys. Rep.* **222**, 145 (1992).
2. Succi, S. *The lattice Boltzmann Equation*, Oxford Science (2001).
3. S. Chen & G. Doolen *Ann. Rev. Fluid Mech.* **30**, 329 (1998).
4. P.L. Bhatnagar, E. Gross & M. Krook *Phys. Rev.* **94**, 511 (1954).
5. X. Shan & H. Chen *Phys. Rev E* **47**, 1815 (1993); *Phys. Rev E* **49**, 2941 (1994).
6. R. Benzi *et al.* *Phys. Rev. E* **74**, 021509 (2006).
7. L. Bocquet & J.-L. Barrat *Phys. Rev. Lett.* **70**, 2726 (1993);
8. P. Thompson & S. Troian *Nature* **389**, 360 (1997).
9. N.V. Priezjev *et al.* *Phys. Rev. E* **71**, 041608 (2005).
10. M. Swift *et al.*, *Phys. Rev. Lett.* **75**, 830, (1995).
11. A. J. Briant *et al.*, *Phil. Trans. R. Soc. Lond. A* **360**, 485, (2002).
12. PHILIP, J. 1972b Integral properties of flows satisfying mixed no-slip and no-shear conditions. *Z. Angew. Math. Phys.* **23**, 960-968.
13. LAUGA, E. & STONE, H. 2003 Effective slip in pressure-driven stokes flow. *J. Fluid.*

6 *R. Benzi, L. Biferale, M. Sbragaglia, S. Succi, F. Toschi*

Mech. **489**, 55.

14. Cottin-Bizonne, C. Barrat, J.-L. Bocquet, L. & Charlaix, E. *Nature Mater.* **2**, 237 (2003).
15. C. Cottin-Bizonne *et al.* *Eur. Phys. J. E* **9**, 47-53 (2002).

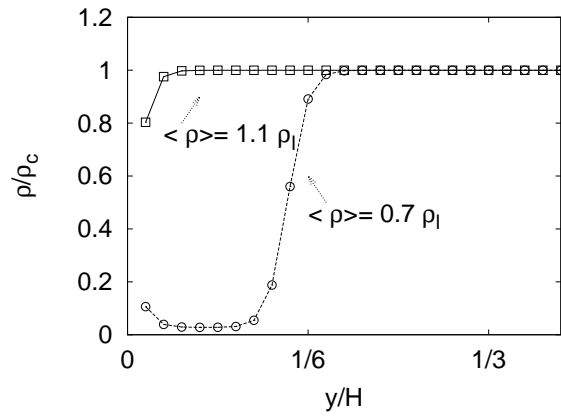


Fig. 1. The stationary state configuration for the density field as a function of the relative distance from the wall, for two different values of the average density of the system: $\langle \rho \rangle = 1.1\rho_l$ (\square) and $\langle \rho \rangle = 0.7\rho_l$ (\circ), where ρ_l is the liquid density. The density tends to match a given value at the wall $\psi(\rho_w = 0.5)$.

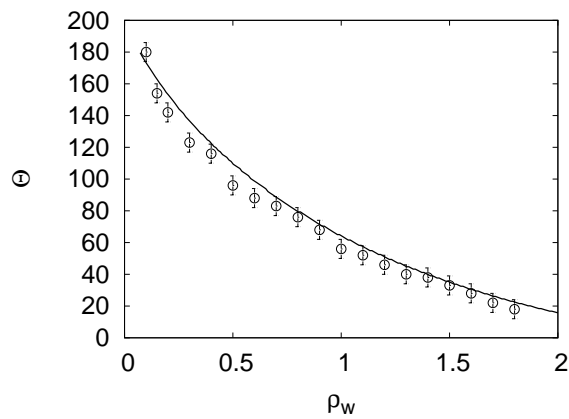


Fig. 2. Contact angle for the case $\mathcal{G}_b = -6.0$ as a function of ρ_w .

8 *R. Benzi, L. Biferale, M. Sbragaglia, S. Succi, F. Toschi*

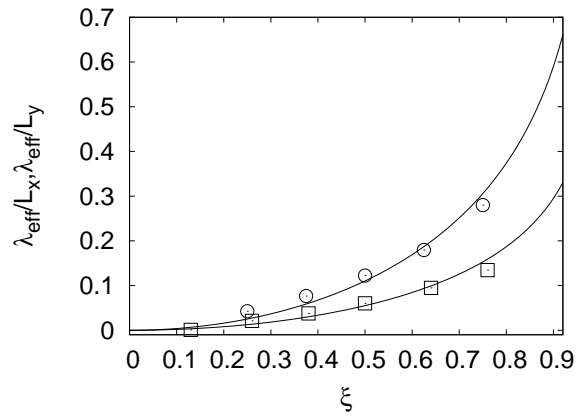


Fig. 3. Numerical results for (ξ) (transversal (\square) and longitudinal (\circ) case) compared against the analytical prediction.

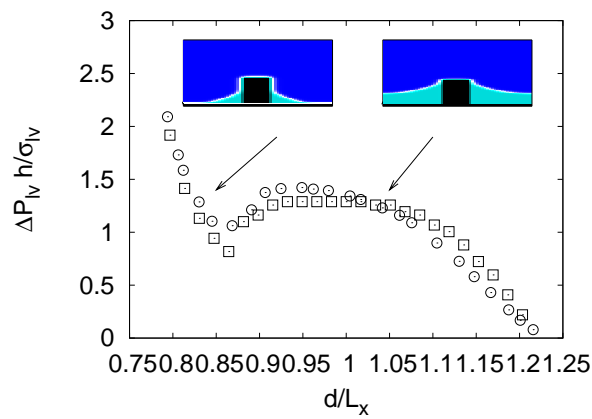


Fig. 4. Validation of LBE (square) simulation against MD (circles), obtained for the same contact angle and the same geometrical properties.

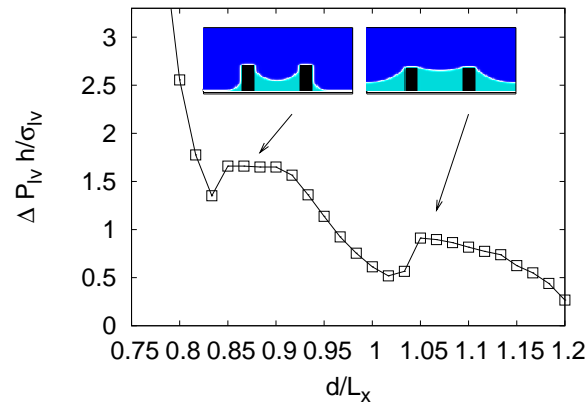


Fig. 5. Pressure variation against the density for the case of heterogeneous roughness.